



Heavy Quark Production at CDF

Mary Bishai (for the CDF Collaboration)

1 Introduction

In QCD perturbation theory, two leading order diagrams are responsible for heavy quark production at hadron colliders, quark-anti quark annihilation, $q\bar{q} \rightarrow Q\bar{Q}$ and gluon fusion, $gg \rightarrow Q\bar{Q}$. In $p\bar{p}$ collisions, the quark cross-sections are convoluted with the parton density functions, $f(x)$, to obtain the hadro-production quark cross-sections as follows:

$$\frac{d\sigma}{dyd\bar{y}dp_T^2} \propto \frac{1}{m_T^4} \frac{1}{[1 + \cosh(y - \bar{y})]^2} \sum_{i,j} x_1 f_i(x_1) x_2 f_j(x_2) \sum_{\bar{}} |M_{ij \rightarrow Q\bar{Q}}|^2 \quad (1)$$

where y and \bar{y} are the produced quark and anti-quark rapidities, and p_T is the transverse momentum. The measurable bottom and charm cross-sections at hadron colliders are of the final hadronic states. The theoretical cross-sections described in Equation 1 are therefore convoluted with the quark fragmentation functions obtained from e^+e^- colliders such as LEP. The inclusive p_T differential cross-sections for charm, bottom and top quarks from the LO QCD calculations are described in [1]. At $\sqrt{s} = 1.8$ TeV, $\sigma(p\bar{p} \rightarrow c\bar{c}) \gg \sigma(p\bar{p} \rightarrow b\bar{b})$ at low p_T and are approximately the same for $p_T \geq 40$ GeV/ c .

In this paper, the CDF Run I bottom and charm quark production results from 118 pb⁻¹ of data collected from 1992 to 1995 during Run I of the Fermilab Tevatron are reviewed and the status of the Run II measurements are presented. Details of top physics results from CDF are presented in [2].

2 Beauty production at CDF

2.1 CDF Run I results

The CDF Run I detector is described in detail in [3]. In Run I, the b quark inclusive cross-sections were measured using the the inclusive $J/\psi, \psi(2s) \rightarrow \mu\mu$ signal from the di-muon triggers with $p_T(\psi) \geq 5$ GeV/ c and pseudo-rapidity range, $|\eta(\psi)| < 0.6$. A fit to the lifetime distribution of the ψ s is used to extract the fraction of $b \rightarrow \psi X$ events and the b hadron inclusive cross-section [4]. The B meson cross-section using the exclusive $B \rightarrow J/\psi K^*$ signal with much smaller statistics was also measured [5]. In addition, the

b hadron inclusive cross-sections were also measured in the modes $b \rightarrow lX$ using data from the high momentum single muon and electron triggers [6].

Initially, the b production cross-sections measured at CDF were more than a factor of two greater than NLO QCD calculations with default parameters [7]. Theory and data could be forced to agree by using extreme values of re-normalization and factorization scales. Recent theoretical advances in the extraction of the non-perturbative fragmentation functions of the B mesons from LEP data in a way that is consistent with the NLO QCD calculations of the hadro-production cross-sections have improved agreement between theoretical predictions and CDF data to better than 50% [8] [9]. Results from CDF Run I and various theoretical predictions are summarized in Figure 1.

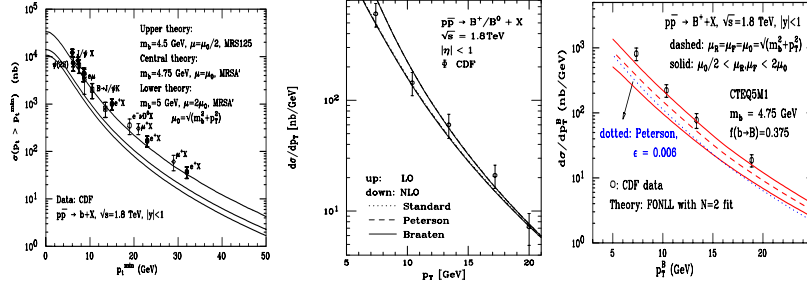


Fig. 1. CDF inclusive b cross-sections with theoretical predictions from [7] (left). B meson cross-sections with theoretical predictions from [8] (center) and [9] (right).

In addition to the flavor creation diagrams discussed in Section 1, two other LO QCD processes contribute to b production in $p\bar{p}$: flavor excitation and shower fragmentation. Tuning contributions from these processes in MC simulations can have a large effect on the total cross-section [10]. To try and estimate the contributions from the 3 processes, $b\bar{b}$ production correlations were studied in Run I. The opening angle in the $r - \phi$ plane between the $b\bar{b}$ hadron pair was examined in a recent analysis of the Run I data using $b\bar{b}$ pairs which decay semileptonically into high p_T leptons and b -jets identified using displaced secondary vertices. The data distribution from $b\bar{b}$ angular correlations, $\Delta\phi(b\bar{b})$, does not agree with the expectations from the LO flavor creation diagram in Pythia, as shown in Figure 2. An excess at smaller opening angles is seen in the data which implies that contributions from flavor excitation and gluon splitting diagrams may be important.

2.2 Preliminary results from CDF Run II

The CDF Run II detector is described in detail in reference [11]. The ψ signals reconstructed from 28 pb^{-1} of data collected from January 2002 to June 2002

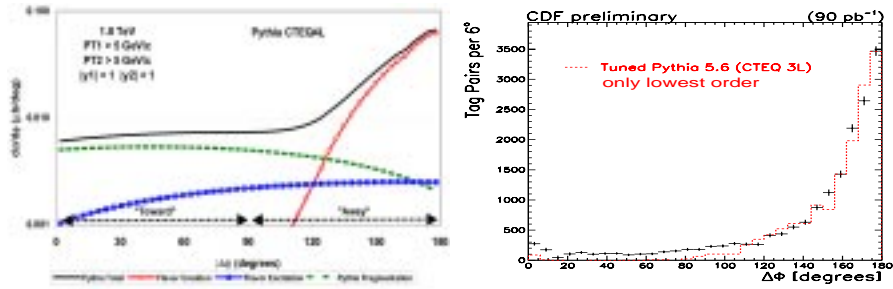


Fig. 2. Opening angle in $r - \phi$ between 2 b quarks in MC (left) and data (right).

are shown in Figure 3. 345,000 $J/\psi \rightarrow \mu\mu$ events and 9,500 $\psi(2s) \rightarrow \mu\mu$ events have been reconstructed. The momentum distribution of J/ψ events in Run II compared to the Run I reach is shown. A fit to the lifetime distribution of a sub-sample of the J/ψ events reconstructed in the SVXII detector is also shown in Figure 3. The fraction of J/ψ from $b \rightarrow J/\psi X$ extracted from the lifetime fit is 17% for events where $p_T(J/\psi) > 4 \text{ GeV}/c$.

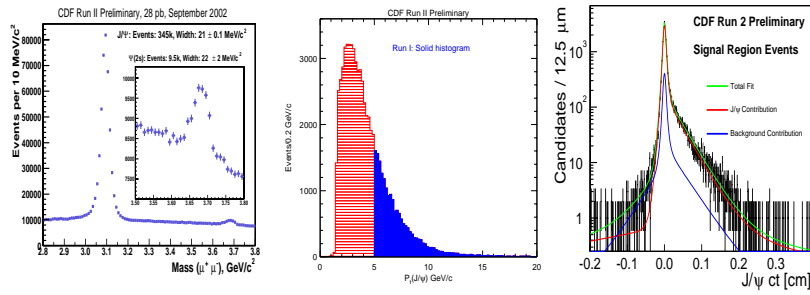


Fig. 3. ψ signals in CDF II (left), the transverse momentum distribution of the J/ψ s in Run II (center), and the fit to the inclusive J/ψ lifetime (right).

Exclusive B mesons in the modes $B_u^+ \rightarrow J/\psi K^+$, $B_d^0 \rightarrow J/\psi K^*$, and $B_s \rightarrow J/\psi \phi$ have also been reconstructed in CDF Run II and are discussed in [12].

The Run II J/ψ and $b \rightarrow J/\psi X$ cross-section measurements from the large statistics samples of inclusive J/ψ s are well under way. Larger statistics of b hadrons reconstructed from exclusive decay modes using triggered J/ψ s are expected by summer 2003.

3 Quarkonia Production at CDF

Non-relativistic quarkonia bound states are best described by Non-Relativistic QCD (NRQCD) theoretical models which are used to predict the hadro-production cross-sections [13]. Predictions using both the color-singlet matrix elements and the higher order, dominant, color-octet matrix elements agree well with data at the Tevatron at high p_T as shown in Figure 4.

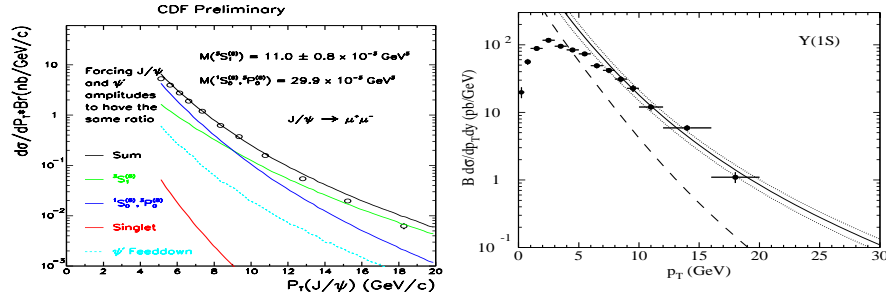


Fig. 4. Direct CDF J/ψ production data and theoretical predictions (left), $Y(1S)$ production (right)

At low momenta, soft gluon effects and non-fragmentation effects from other octet matrix elements that are difficult to calculate theoretically become important and cause theory predictions and data to diverge. The NRQCD color octet matrix elements can be determined by fitting to the measured Run I CDF cross-sections of $Y(nS)$ for $p_T(Y) > 8 \text{ GeV}/c$, where $n = 1, 2, 3$ and the P-wave states $\chi_b(1P)$ and $\chi_b(2P)$. Using the color octet matrix elements derived from data, $\sigma(\eta_b(1S)X)/\sigma(Y(1S)X) \sim 4.3$ is predicted [14]. From 80 pb^{-1} of Run I data, 7 candidate events of $\eta_b \rightarrow J/\psi J/\psi$ were observed with a potential mass of $9446 \pm 6(\text{stat}) \text{ MeV}/c^2$. The large J/ψ statistics from Run II will confirm the observation of the η_b and the relative branching fraction to the $Y(1S)$ can be measured and compared to theoretical predictions. The Run I $\eta_b \rightarrow J/\psi J/\psi$ potential signal and the Run II $Y(nS) \rightarrow \mu\mu$ invariant mass distributions are shown in Figure 5.

Inclusion of the color octet in NRQCD leads to a prediction of increasing transverse polarization of charmonium at high p_t [15]. The polarization parameter, α , is obtained from an unbinned likelihood fit to the production angle distribution of the Run I J/ψ events using a weighed MC distribution which is a mixture of transverse and longitudinal polarizations. A simultaneous fit to the J/ψ lifetime separates prompt J/ψ events from $b \rightarrow J/\psi X$ [16]. The distribution of the α values thus obtained as a function of p_T of the J/ψ are shown in Figure 6. In the Run I data, α is positive at intermediate p_T but does not continue to rise at high p_T as predicted by theory.

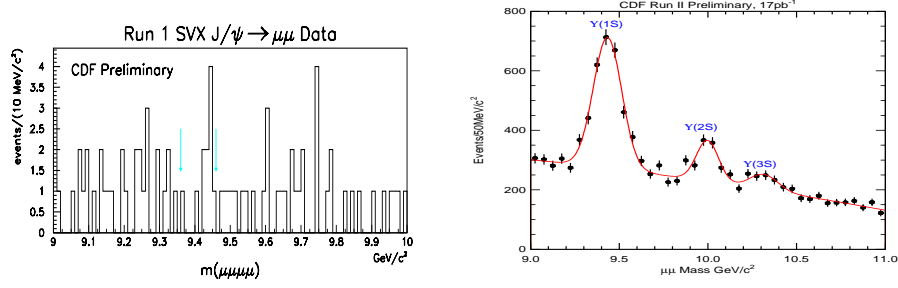


Fig. 5. Run I $\eta_b \rightarrow J/\psi J/\psi$ candidate events (left). Run II $\Upsilon(ns)$ signals (right).

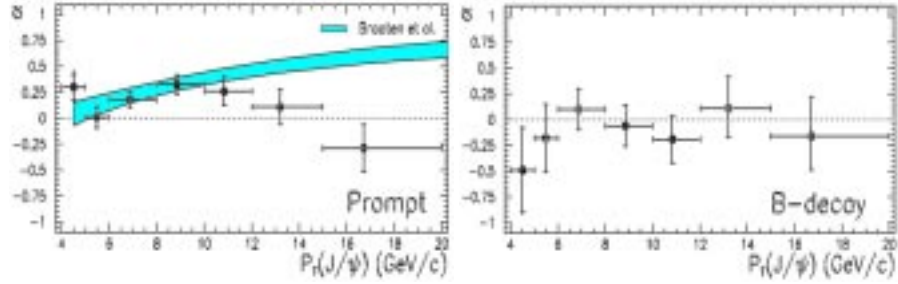


Fig. 6. The distribution of the polarization parameter, α , as a function of p_T of the J/ψ for prompt (left) and $b \rightarrow J/\psi$ (right) events. The NRQCD prediction is the shaded band shown on the left plot.

4 Charm Production at CDF

4.1 Run I results

The D^* direct production cross-section was measured in the CDF run I data using the inclusive muon triggers with $p_T(\mu) > 7.5$ GeV/c where the D^* is reconstructed from the decay chain $D^* \rightarrow D^0 \pi_s$, $D^0 \rightarrow K \mu + X$. A fit to the D^0 decay vertex lifetime is used to extract the fraction of D^* from B mesons. The B fraction measured is relatively small and is found to be $< 6.5\%$. Using the charm quark branching fraction, $c \rightarrow D^{*+} = 0.222$, charm quark mass of 1.5 GeV/c², and a charm Peterson fragmentation function with $\epsilon_q = 0.02$ [17], the total expected theoretical cross-section from NLO QCD is $\sigma(p\bar{p} \rightarrow D^* X)_{theory} = 240$ nb. The total cross-section measured in data is found to be higher, $\sigma(p\bar{p} \rightarrow D^* X)(|\eta| < 1.0, p_T > 10 \text{ GeV}) = 347 \pm 65(stat) \pm 58(syst)$ nb. The transverse momentum spectrum also falls more rapidly than the theoretical prediction (Figure 7).

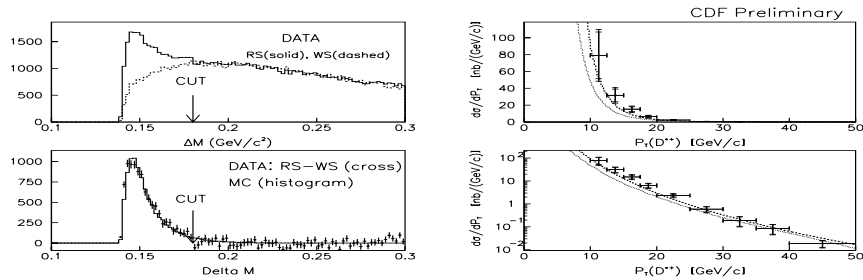


Fig. 7. Run I $D^* - D^0$ Mass difference (left) and differential cross-section (right).

4.2 Run II charm production cross-sections

In CDF Run II, the Silicon Vertex Tracker (SVT) [18] reconstructs 2-D tracks in the SVXII online, thus allowing triggers on detached vertices at level 2. Since January 2002, large samples of D and B mesons from $B \rightarrow DX$ decays have been collected using SVT [12].

To estimate the fraction of D mesons from $B \rightarrow DX$ decays, f_b , an unbinned likelihood fit to the impact parameter, d_0 , of the reconstructed D meson measured with respect to the primary vertex is performed. D mesons from long lived B decays have large impact parameters when compared to prompt D s. The shape of the impact parameter distribution of SVT triggered D s from B decays, $F_B(d_0)$, is modeled using a Monte Carlo simulation. The detector d_0 resolution, $F_D(d_0)$, is calibrated using prompt $K_s \rightarrow \pi\pi$ events with the same selection criteria as $D \rightarrow K^-\pi^+$. The fit functional form is :

$$F(d_0) = f_B \int F_B(x)F_D(d_0 - x)dx + (1 - f_B)F_D(d_0) \quad (2)$$

The fit results are shown in Figure 8. The fraction of D s from $B \rightarrow D$ decays is measured to be $\approx 16\%$ for D^0 , 11% for $D^{+,*+}$ and 35% for D_s .

5 Conclusion

Heavy quark production cross-sections, correlations and polarizations have been measured at the Collider Detector at Fermilab (CDF) using 118 pb^{-1} of data collected from the 1992 to 1995 Run I of the Fermilab Tevatron. There is still disagreement between theoretical predictions of bottom and charm hadro-production cross-sections and the Run I results. The observed transverse momentum spectrum of the prompt J/ψ production polarization is still not understood.

Run II of the Tevatron began in July of 2001 and the CDF Run II detector [11] has collected 70 pb^{-1} of physics quality data since January 2002. Large

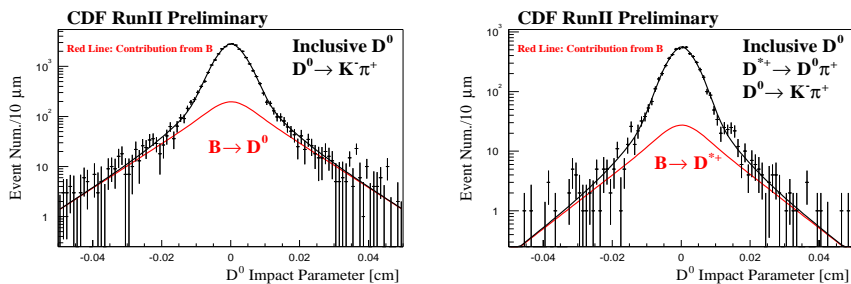


Fig. 8. Fit to the impact parameter distribution of the D^0 (left) and D^* (right) candidates. Red line shows the contribution from $B \rightarrow D^{0,*} X$.

statistics of onia states have been collected. Exclusive B meson decay modes have been reconstructed and the SVT level 2 displaced track trigger has produced large samples of D mesons. The prompt charm and $b \rightarrow cX$ fractions in both charmonium and D meson samples have been measured. Run II is now poised to greatly enhance the knowledge of heavy quark production dynamics well beyond the reach of the Run I detector.

References

1. Michelangelo L. Mangano, hep-ph/9711337 (1997).
2. Wolfgang Wagner, *Top Physics with CDF*, these proceedings.
3. CDF Collaboration, F. Abe *et al.*, Nucl. Instrum. Methods Phys. Res. Sect. A **271** 376 (1988).
4. CDF Collaboration. F.Abe *et al.*, Phys.Rev.Lett. **79**, 572 (1997).
5. CDF Collaboration. F.Abe *et al.*, Phys.Rev.Lett. **75**, 1451 (1995).
6. CDF Collaboration. F.Abe *et al.*, Phys.Rev.Lett. **71**, 2396 (1993)
CDF Collaboration. F.Abe *et al.*, Phys.Rev.Lett. **71**, 500 (1993)
7. P. Nason, S. Dawson and R. K. Ellis, Nucl. Phys. **B 303**, 607 (1988).
P. Nason *et al.*, Nucl. Phys. **B 327**, 49 (1989), erratum-ibid **B 335** 260 (1989).
W. Beenakker *et al.*, Nucl. Phys. **B 351**, 507 (1991).
8. J. Binnewies, Bernd A. Kniehl and G. Kramer, Phys. Rev. D58 034016 (1998).
9. Matteo Cacciari and Paolo Nason, Phys. Rev. Lett. 89 122003 (2002).
10. R.D. Field, Phys. Rev. **D 65** 094006 (2002).
11. Frank Chlebana, *Status of the CDF Run II Detector*, these proceedings.
12. Sandro DeCecco, *B-mass, lifetimes, ...*, these proceedings.
13. Adam K. Leibovich, Nucl. Phys. Proc. Suppl. **93** 182 (2001).
14. Eric Braaten, Sean Fleming, Adam Leibovich, Phys. Rev. **D 63** 094006 (2001).
15. P. Cho and M. Wise, Phys. Lett. **B 346**, 129 (1995).
M. Beneke and M. Krämer, Phys. Rev. **D 55**, 5269 (1997).
Eric Braaten, Bernd A. Kniehl and Jungil Lee, Phys. Rev. **D 62** 094005 (2000)
16. CDF Collaboration. T. Affolder *et al.*, Phys. Rev. Lett. **85** 2886 (2000).
17. Matteo Cacciari, hep-ph/9708282
18. A. Bardi *et al.*, Nucl. Instrum. Meth. **A 485** 178 (2002).